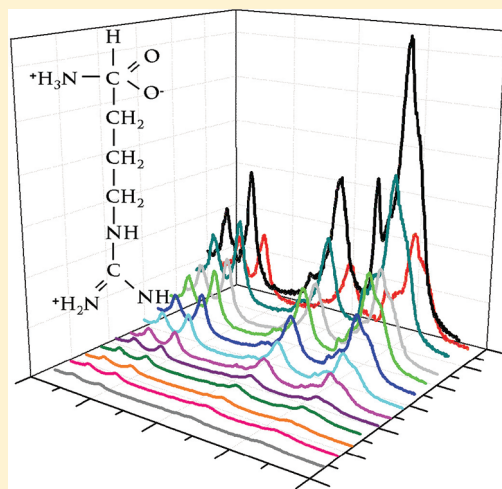


UV Resonance Raman Finds Peptide Bond–Arg Side Chain Electronic Interactions

Bhavya Sharma and Sanford A. Asher*

Department of Chemistry, University of Pittsburgh, 219 Parkman Avenue, Pittsburgh, Pennsylvania 15260, United States

ABSTRACT: We measured the UV resonance Raman excitation profiles and Raman depolarization ratios of the arginine (Arg) vibrations of the amino acid monomer as well as Arg in the 21-residue predominantly alanine peptide AAAA(AAARA)₃A (AP) between 194 and 218 nm. Excitation within the $\pi \rightarrow \pi^*$ peptide bond electronic transitions result in UVRR spectra dominated by amide peptide bond vibrations. The Raman cross sections and excitation profiles indicate that the Arg side chain electronic transitions mix with the AP peptide bond electronic transitions. The Arg Raman bands in AP exhibit Raman excitation profiles similar to those of the amide bands in AP which are conformation specific. These Arg excitation profiles distinctly differ from the Arg monomer. The Raman depolarization ratios of Arg in monomeric solution are quite simple with $\rho = 0.33$ indicating enhancement by a single electronic transition. In contrast, we see very complex depolarization ratios of Arg in AP that indicate that the Arg residues are resonance enhanced by multiple electronic transitions.



INTRODUCTION

There is little understanding of the electronic transitions of peptides and proteins.^{1–10} It is generally assumed that peptide and protein electronic transitions result from the summation of the electronic transitions of the constituent chromophores. The peptide bond $\pi \rightarrow \pi^*$ transitions have been characterized to a limited extent, as have been the transitions of the different isolated side chain chromophores.^{1–13} However, there has been little attention paid to the potential coupling of the peptide bond transitions to the side chain electronic transitions or to coupling between side chain transitions. Coupling of side chain–peptide bond transitions could be important in areas such as electron transport, for example.

In the work here, we use UV resonance Raman (UVRR) spectroscopy^{14–28} to probe the electronic transitions of Arg side chains in a predominantly poly-Ala peptide. UVRR spectroscopy is unique in its ability to provide insight into the electronic excited state geometry and the localization of electronic transitions through measurements of Raman excitation profiles and Raman depolarization ratios.^{24,25,29–37}

We examined the excitation profiles of the three Arg residues within a 21-residue, primarily poly-Ala peptide (AP), which has been well characterized and used as a model for α -helix conformations and α -helix melting. AP has previously been shown to be in an α -helical conformation at low temperatures that melts to a predominantly poly-proline II-like (PPII) conformation at high temperatures.^{15,19,21,22,25} Excitation between 180 and 215 nm occurs in resonance with the peptide bond $\pi \rightarrow \pi^*$ electronic transitions,

resulting in enhancement of amide vibrations.^{14–17,19–22,24,25,28–38} We show here that the electronic transitions of the Arg side chains strongly couple to the $\pi \rightarrow \pi^*$ peptide bond electronic transitions.

MATERIALS AND METHODS

Sample Preparation. The 21-residue poly-alanine peptide AAAA(AAARA)₃A (AP) was prepared by AnaSpec (San Jose, CA) using solid-state peptide synthesis (HPLC pure). We used 2 mg/mL (1.13 mM) AP solutions that contained sodium perchlorate (0.2 M) as an internal standard for the UVRRS measurements. The Arg HCl (Arg) (Sigma; St. Louis, MO) UVRRS measurements used 2 mg/mL (9.7×10^{-3} M) solutions with sodium perchlorate (0.2 M) as an internal standard. The UVRR spectral measurements of Arg were taken at 25 ± 0.5 °C. The AP UVRR spectral measurements were measured at both 5 ± 0.5 °C (where AP is a mixture of α -helical and PPII conformations) and 60 ± 0.5 °C (where the PPII-like conformation dominates) (Figure 1). All UVRRS and absorption spectra of AP and Arg were measured at pH 7.

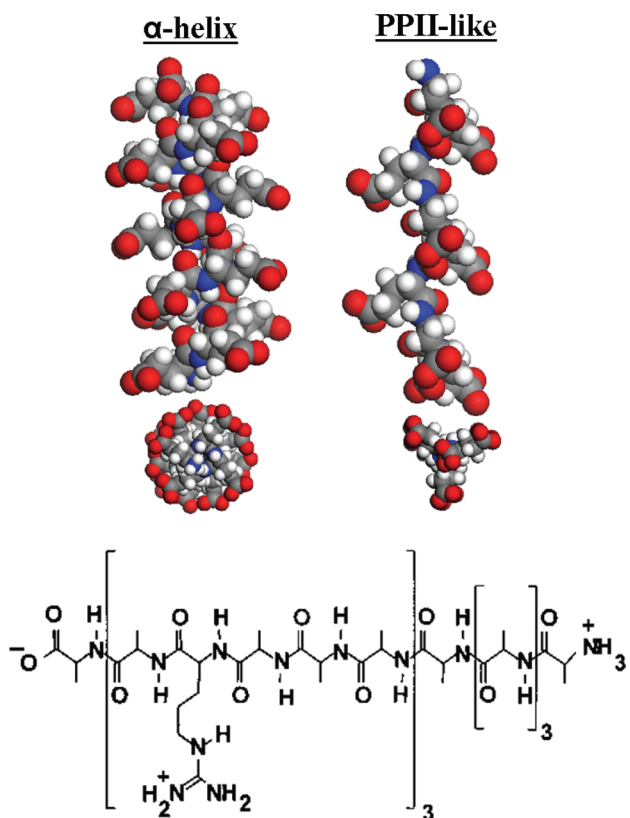
Raman Instrumentation. The UVRR instrumentation was previously described in detail.³⁹ The excitation profile measurements utilize two Coherent Indigo-S Ti:sapphire laser systems to

Special Issue: Shaul Mukamel Festschrift

Received: December 22, 2010

Revised: February 28, 2011

Published: March 16, 2011



span the spectral region of interest. Both lasers utilize intracavity frequency doubled, Q-switch pulsed Nd:YLF Evolution 15 lasers (527 nm wavelength, 5 kHz repetition rate, 10 W average power) to pump Ti:sapphire oscillators generating tunable radiation from 772 to 840 nm and from 840 to 960 nm. These tunable Ti:sapphire lasers are frequency quadrupled and mixed, utilizing two different harmonic generation approaches. The first laser uses two successive frequency doublers to convert the fundamental wavelengths (840–960 nm) to the deep UV (210–240 nm). The second harmonic generation process mixes the third harmonic with the fundamental to produce tunable radiation between 193 and 210 nm. The average powers in the UV are between 2 and 5 mW (193–210 nm) and between 2 and 10 mW (210–220 nm).

The laser beam is focused into a temperature-controlled, circulating flow stream which was surrounded by a N_2 gas environment, thereby eliminating Raman scattering from the O_2 Raman band at 1555 cm^{-1} . Each 20 mL sample of AP or Arg was irradiated for a maximum of 15 min. The scattered light was directed into a subtractive double monochromator,³⁹ and the Raman scattered light was detected by a liquid nitrogen cooled CCD (Princeton Instruments, Spec-10:400B). The Raman intensities were normalized to the 932 cm^{-1} perchlorate ClO_4^- symmetric stretch vibration. The spectra were analyzed and deconvoluted using Grams/32 AI 8.0 software (Thermo Electron Corporation, Waltham, MA).

UV Raman depolarization ratios (ρ) were measured by using a backscattering geometry. The light scattered from the sample was directed through a UV linear dichroic polarizer (Oriel

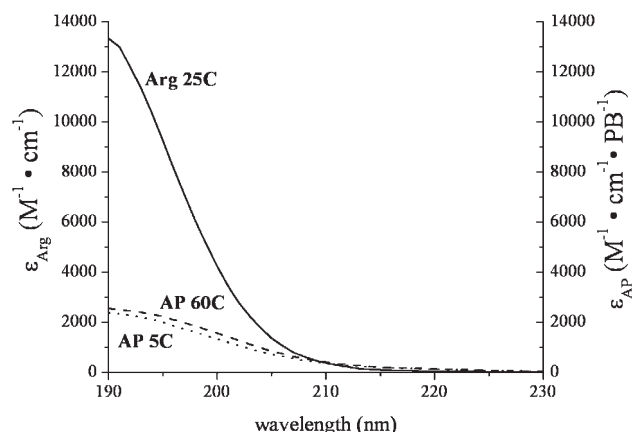


Figure 2. UV absorption spectrum of Arg at pH 7 and $25\text{ }^\circ\text{C}$; UV absorption spectra of AP at $5\text{ }^\circ\text{C}$, where it is predominantly α -helical, and at $60\text{ }^\circ\text{C}$, where it is predominantly in a PPII-like conformation.

Instruments, Stratford, CT) and a crystalline quartz scrambler (Spex Industries, Edison, NJ) placed directly before the monochromator entrance slit. The depolarization ratios were measured between 198 and 218 nm and at 229 nm. The incident beams were highly polarized. ρ was calculated as the ratio of the perpendicularly polarized (I_{\perp}) to the parallel polarized scattered light (I_{\parallel}):

$$\rho = \frac{I_{\perp}}{I_{\parallel}} \quad (1)$$

The depolarization ratios were calibrated by using the depolarization ratios of ClO_4^- and cyclohexane as standards.³⁵

Spectrometer Efficiency. The spectrometer used is a modified Spex 1401 double monochromator that operates in the 193–270 nm range. The throughput efficiency of the spectrometer varies over this range. We corrected for the differences in throughput by using previously determined efficiency measurements.³⁹

Absorption Measurement. The UV absorbance spectra between 190 and 260 nm were measured by using a Cary 5000 Varian UV-vis-NIR spectrophotometer. The Arg solution concentration used for the absorbance measurements was $3.4 \times 10^{-4}\text{ M}$. The absorbance measurements for the Arg samples were taken at $25 \pm 0.5\text{ }^\circ\text{C}$. The AP absorption measurements used 0.15 mM concentrations at temperatures of 5 ± 0.5 and $60 \pm 0.5\text{ }^\circ\text{C}$.

■ RESULTS AND DISCUSSION

Absorption Spectra. Figure 2 shows the absorption spectra of AP and Arg. The broad bands at 190 nm of the AP samples derive from the peptide bond $\pi \rightarrow \pi^*$ transitions, while the band from the Arg monomer derives from the two lowest $\pi \rightarrow \pi^*$ transitions of the guanidinium group.⁴⁰ These guanidinium electronic transitions have been calculated to be at 199 and 185 nm by Sension et al.⁴⁰ These authors, however, have further stated that the calculated energy values are probably too low by $3000\text{--}6000\text{ cm}^{-1}$, and the transitions are more likely to be at 177–188 and 166–175 nm. The Figure 2 absorption spectrum does not show discrete peaks for the transitions, presumably because it does not go to short enough wavelengths. We previously showed that AP at both low and high temperatures shows excitonic

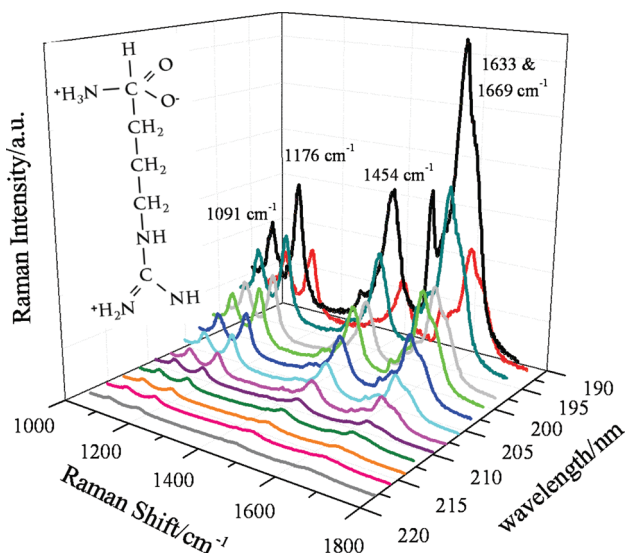


Figure 3. UVRR spectra of Arg at 25 °C between 218 and 194 nm. The spectra were collected for 15 min at each excitation wavelength. The spectral resolution varies between 5.9 cm^{-1} at 218 nm and 7 cm^{-1} at 194 nm. All spectra were normalized to the ClO_4^- internal standard (not shown). Inset: Arg structure.

interactions between the peptide bond $\text{NV}_1\pi \rightarrow \pi^*$ transitions and higher energy transitions that impact the peptide bond absorption band.²⁵

UVRR Spectra of Arg. The UVRRS of Arg at 25 °C excited between 218 and 194 nm are shown in Figure 3. The spectra are normalized with respect to the 932 cm^{-1} ClO_4^- band (not shown) but are not corrected for self-absorption or spectrometer efficiency. The UV Raman enhanced Arg vibrations include the guanidinium group overlapping 1669 and 1633 cm^{-1} bands, which arise primarily from CN stretching (st), NH₂ scissoring (sci), and NH bending (b) vibrations.^{41–44} The 1565 cm^{-1} band is due to NH₂ sci, and is only present in spectra excited below 200 nm.⁴⁰ The 1454 cm^{-1} band is due to CH₂ sci.^{42,43} The 1176 cm^{-1} band results from CH₂ twisting (tw), CH b, and NH₂ tw of the guanidinium group.^{42,43,45} The 1091 cm^{-1} band is due primarily to a NH₂ rocking (rock) vibration of the guanidinium group with NH₂ wagging (w), CH₂ w, and CH b.^{42,43,45} The relative intensities of the UVRR bands of Arg increase as the excitation wavelength decreases from 218 to 196 nm (Figure 3), but the intensity decreases for 194 nm excitation.

The 204 nm UVRR spectra of AP in the PPII-like and α -helix conformations are shown in Figure 4 with the Arg bands labeled. The UVRR spectra of the PPII-like and α -helical AP conformations significantly differ, as do their excitation profiles.²⁵ The Arg bands at 1091 , 1176 , and 1454 cm^{-1} are clearly evident. The 1600 – 1670 cm^{-1} region Arg bands underlie the amide I band but by modeling can be resolved.

Absolute Raman Cross Sections. We calculated the Raman cross sections of the Arg bands in solution and the Arg bands in AP by using ClO_4^- as an internal standard. We previously showed that the ClO_4^- Raman cross section dependence on excitation wavelength is well modeled by an Albrecht A-term frequency dependence for excitation wavelengths from the visible to the UV to 220 nm:¹⁸

$$\sigma_R = K_2(\nu_o - \nu_{mn})^3 \left[\frac{\nu_e^2 + \nu_o^2}{\nu_e^2 - \nu_o^2} \right]^2 \quad (2)$$

where K_2 is a constant equal to $2.34 \times 10^{-26}\text{ cm}^2/\text{mol} \cdot \text{sr}$, ν_o is the

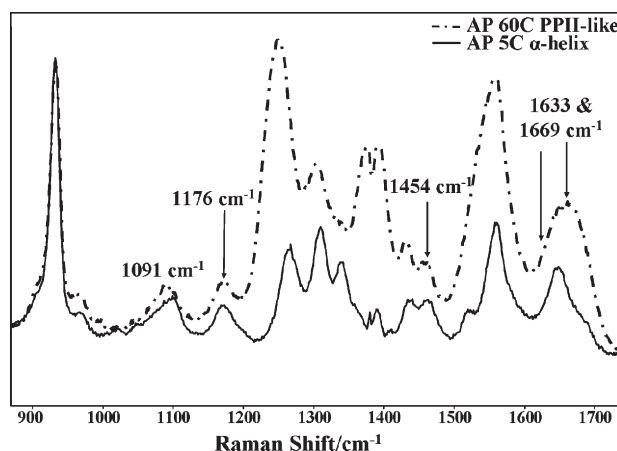


Figure 4. UVRR spectra of AP (pH 7) at 60 °C and 5 °C excited at 204 nm. The spectra were collected for 15 min at each excitation wavelength. The Arg bands in the AP spectra are labeled.

incident laser excitation frequency (cm^{-1}), ν_{mn} is the frequency of the Raman vibrational mode (cm^{-1}), and ν_e is the frequency of the transition to the resonant excited state ($1.28 \times 10^5\text{ cm}^{-1}$). We assume this cross section frequency dependence occurs down to 194 nm.^{24,25}

We normalized all of the UVRR spectra to the integrated intensity of the ClO_4^- 932 cm^{-1} band. The absolute Raman cross sections (with correction for self-absorption) of the Arg bands in both conformations of AP and for pure Arg in solution were calculated as

$$\sigma_R = \frac{I_{\text{band}} \cdot k(\lambda_{\text{ClO}_4}) \cdot C_{\text{ClO}_4} \cdot \sigma_{\text{ClO}_4}}{I_{\text{ClO}_4} \cdot k(\lambda_{\text{band}}) \cdot C_{\text{sample}} \cdot n_{\text{Arg}}} \cdot \left[\frac{\varepsilon_s + \varepsilon_o}{\varepsilon_r + \varepsilon_o} \right] \quad (3)$$

where I_{band} and I_{ClO_4} are the observed integrated intensities of the Arg and ClO_4^- bands, respectively; $k(\lambda_{\text{band}})$ and $k(\lambda_{\text{ClO}_4})$ are the spectrometer efficiencies at the specific wavelengths of the Raman bands; C_{sample} and C_{ClO_4} are the concentrations (M) of the AP or Arg samples and perchlorate; σ_{ClO_4} is the calculated ClO_4^- cross section at the excitation wavelength; n_{Arg} is the number of Arg residues in AP; ε_o is the extinction coefficient for AP at the excitation frequency; ε_s is the extinction coefficient for AP at each Raman band wavelength; and ε_r is the extinction coefficient for the ClO_4^- band at each excitation wavelength. The expression in the brackets corrects the Raman intensities for self-absorption.^{24,25,46,47}

Excitation Profiles of Arg in Solution. Figure 5a shows the Raman excitation profile cross sections of Arg in solution. The excitation profile cross sections increase from 218 to 194 nm, reaching a maximum at 196 nm, and then decrease. The excitation profiles are all significantly narrower than is the Arg absorption spectrum (Figure 5). These Arg monomer excitation profile maxima, which should signal a guanidinium group $\pi \rightarrow \pi^*$ transition, appear at lower energy than the calculated lowest energy transitions for the guanidinium group (<188 nm).⁴⁰ Thus, our Raman excitation profile data are not consistent with Sension et al.'s calculations and indicate that the lowest $\pi \rightarrow \pi^*$ transition of Arg occurs at 196 nm. The 1091 (NH₂ rock, NH₂ w, CH₂ w, and CH b), 1176 (CH₂ twist, CH b, and NH₂ tw), 1454 (CH₂ sci), and 1633 (CN st, NH₂ sci, NH b) cm^{-1} vibrations have similar excitation profiles between 198 and 218 nm. There

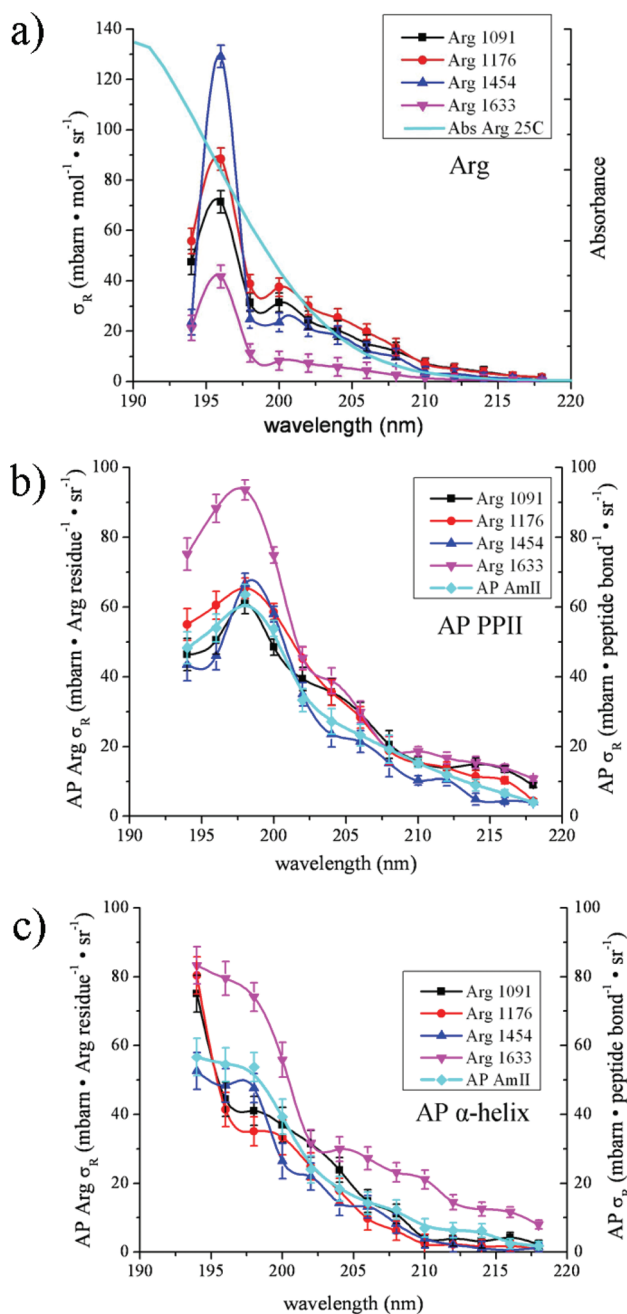


Figure 5. (a) Absolute Raman cross section ($\text{mbarn} \cdot \text{mol}^{-1} \cdot \text{sr}^{-1}$) excitation profiles between 194 and 218 nm of Arg in solution at 25 °C. Also shown is the Arg absorption spectrum. (b) Absolute Raman cross section excitation profiles ($\text{mbarn} \cdot \text{Arg residue}^{-1} \cdot \text{sr}^{-1}$) of Arg vibrations in the PPII-like conformation of AP, and the AP AmII Raman cross section excitation profile ($\text{mbarn} \cdot \text{peptide bond}^{-1} \cdot \text{sr}^{-1}$) of the PPII-like conformation. (c) Absolute Raman cross section excitation profiles ($\text{mbarn} \cdot \text{Arg residue}^{-1} \cdot \text{sr}^{-1}$) of the Arg vibrations of the α -helix conformation of AP, and the α -helix conformation AP peptide bond AmII Raman cross section excitation profile ($\text{mbarn} \cdot \text{peptide bond}^{-1} \cdot \text{sr}^{-1}$).

appears to be a shoulder between 200 and 210 nm in the Arg excitation profiles.

Recent studies by our group on the absorption spectrum of ethylguanidinium, that has the same local guanidinium group

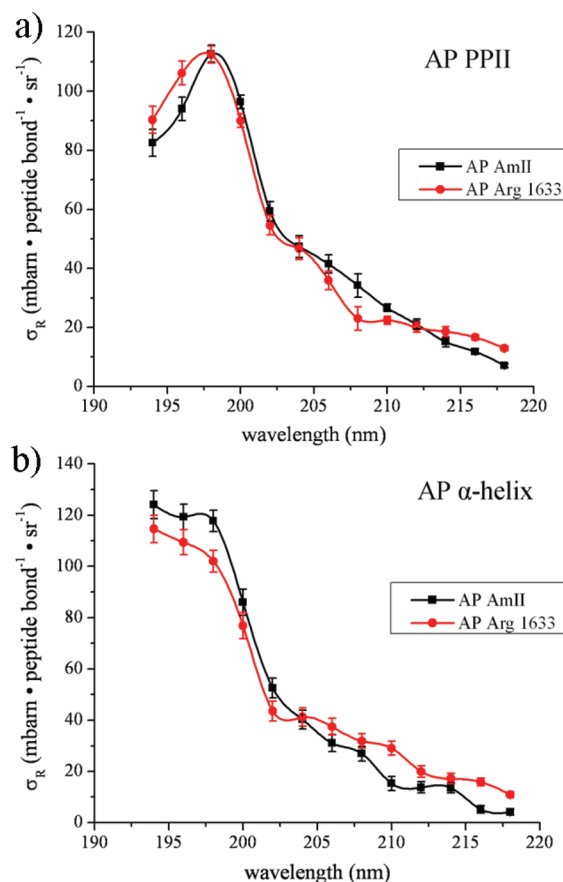


Figure 6. Overlapped ($\text{mbarn} \cdot \text{peptide bond}^{-1} \cdot \text{sr}^{-1}$) cross sections of (a) the AP AmII vibration and Arg 1633 cm^{-1} band in the AP PPII-like conformation and (b) the AP AmII vibration and Arg 1633 cm^{-1} band in the AP α -helix conformation.

symmetry and the same vibrational spectra above $\sim 1000 \text{ cm}^{-1}$ as the Arg side chain, indicates the existence of a broad underlying transition centered between 200 and 210 nm.⁴⁸

Excitation Profiles of Arg in AP. Figure 5b and c shows the Raman cross section excitation profiles of the 1091, 1176, 1454, and 1633 cm^{-1} Arg bands observed in the UVRR spectra of AP in both the PPII and α -helix conformations, along with the AP peptide bond AmII vibration which has an excitation profile similar to those of other peptide bond amide vibrations.

The excitation profiles of the Arg residues in both conformations of AP (Figure 5b and c) significantly differ from the excitation profiles of pure Arg in solution (Figure 5a). Remarkably, and quite unexpectedly, the AP PPII Arg and the α -helix Arg bands have the same excitation profiles as the peptide bonds in both the AP PPII-like and α -helix conformations. The cross sections of the AP Arg bands (per Arg residue) are similar to those of the AmII vibration (per peptide bond; Figure 5b and c). This is most clearly evident in Figure 6.

The essentially identical Raman excitation profiles of the Arg and peptide bond vibrations in AP clearly indicate mixing between the overlapping Arg guanidinium group electronic transitions and those of the peptide backbone.

Depolarization Ratios. To further explore the electronic interactions between the AP peptide backbone and Arg side chains, we measured the dispersions of the UVRR depolarization ratios of the Arg bands in AP. The value of ρ can be used to signal

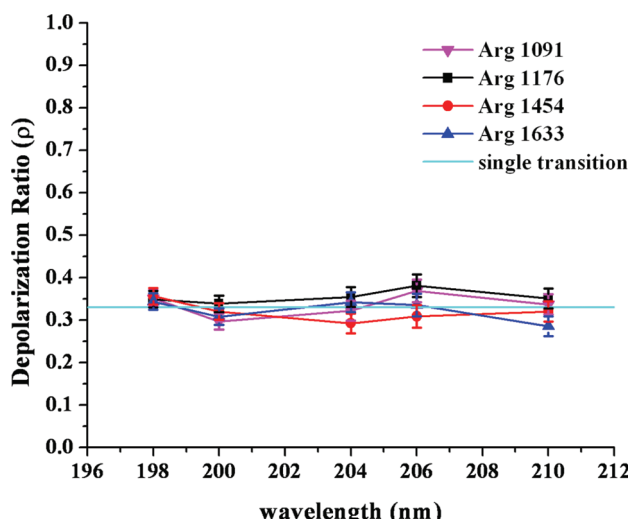


Figure 7. Depolarization ratios of Arg in water. These $\rho = 0.33$ values indicate the occurrence of a single electronic transition.

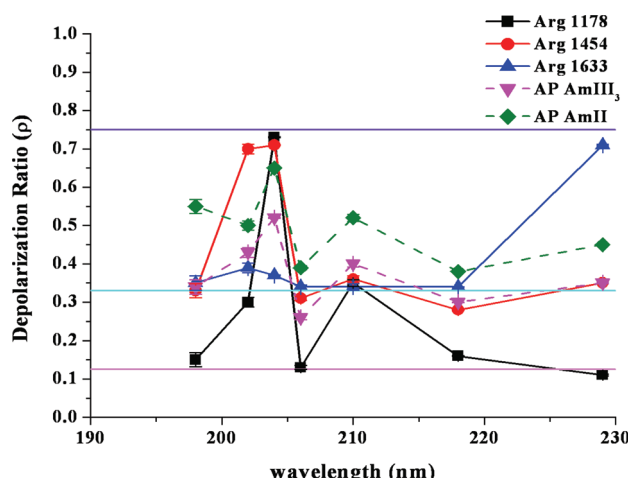


Figure 8. Depolarization ratios of the Arg vibrations and of two AP amide vibrations in the PPII-like conformation of AP: single electronic transitions $\rho = 0.33$ (aqua), totally nonsymmetric transitions $\rho = 0.75$ (purple), and totally symmetric transitions $\rho = 0.125$ (pink). ρ values are indicated by solid lines.

the existence of electronic transitions underlying broad absorption bands. A resonance Raman depolarization ratio of $\rho = 0.33$ indicates that only a single, nondegenerate electronic transition contributes to the resonance Raman tensor elements.^{24,25,31,32,49} When $\rho \neq 0.33$, the resonance enhancement arises from at least two electronic transitions contributing to the Raman tensor. If $\rho > 0.33$, and if there are only two diagonal elements of the Raman tensor, they must be of opposite sign. For $\rho < 0.33$, where only two diagonal elements contribute, the two diagonal elements must be of the same sign.^{24,25,31,32,49} Thus, $\rho \neq 0.33$ requires the contribution of at least two electronic transitions.

In resonance Raman, $\rho = 0.75$ indicates a totally nonsymmetric vibration, while $\rho = 0.125$ indicates two identical Raman tensor elements that could result from a doubly degenerate resonant electronic transition.⁴⁹

For Arg in solution, with $\rho = 0.33$, the excitation wavelength independence of the depolarization ratios indicates that a single

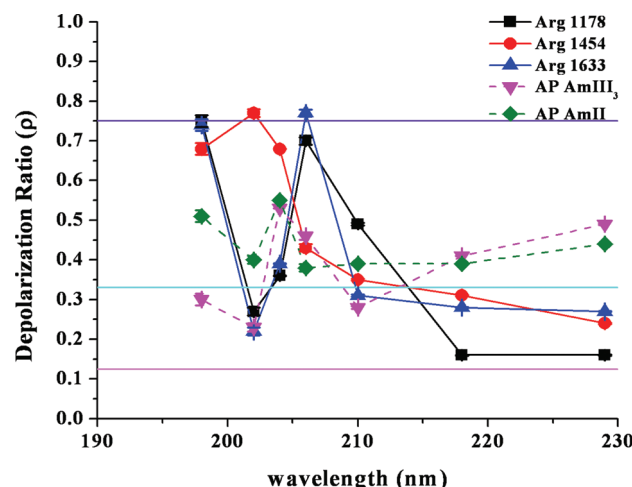


Figure 9. Depolarization ratios for the Arg vibrations and for two AP amide vibrations in the α -helix conformation of AP: single electronic transitions $\rho = 0.33$ (aqua), totally nonsymmetric transitions $\rho = 0.75$ (purple), and doubly degenerate symmetric transitions $\rho = 0.125$ (pink). ρ values are indicated by solid lines.

electronic transition dominates the enhancement for this excitation frequency region (Figure 7). This presumably is the lower energy $\pi \rightarrow \pi^*$ transition of the substituted guanidinium group. This alkyl guanidinium substitution breaks the symmetry of the normally degenerate guanidinium group $\pi \rightarrow \pi^*$ symmetry,⁴⁰ splitting the transition.

Figures 8 and 9 show the depolarization ratios of the 1178, 1454, and 1633 cm^{-1} AP Arg bands, as well as two amide peptide bond vibrations of the AmIII₃ and AmII in the PPII-like (Figure 8) and α -helix (Figure 9) conformations. For both conformations, we find that there is a complex dispersion of the depolarization ratio with variation in the excitation wavelength. For the PPII-like conformation (Figure 8), we see that, although both the AP AmIII₃ and AmII vibrations have depolarization ratios above $\rho = 0.33$, the ratios do not go above $\rho = 0.65$, with four of the AmIII₃ ρ values at or below $\rho = 0.33$ (at $\lambda_{\text{ex}} = 198$, 206, 218, and 229 nm). The AP Arg vibrations however reach values of both $\rho = 0.125$ and $\rho = 0.75$ for several wavelengths.

These depolarization values indicate contributions of multiple electronic transitions. For the α -helix conformation (Figure 9), we see a similar depolarization ratio pattern for the Arg vibrations. Further, the UV resonance Raman excitation profiles and Raman depolarization ratios indicate that the electronic transitions of the Arg side chains in the peptide AP distinctly differ for those of pure Arg in solution. The results clearly show that the Arg side chains in AP undergo electronic interactions with the overlapping peptide bond $\pi \rightarrow \pi^*$ electronic transitions of the peptide backbone.

CONCLUSIONS

We measured the UV resonance Raman excitation profiles and depolarization ratios for the Arg residues attached to the peptide AP and for Arg in solution. We find that the resonance Raman excitation profiles of the Arg in both the α -helix and PPII-like conformations of AP are essentially identical to those of the amide peptide bond bands. These excitation profiles are distinctly different from the excitation profiles of the monomeric Arg amino acid in solution. The excitation profile similarities

must result from interactions of the Arg side chain electronic transitions with the peptide backbone amide $\pi \rightarrow \pi^*$ transition.

We show that the depolarization ratios of the Arg monomer amino acid in water indicate that a single electronic transition dominates for excitation between 198 and 210 nm. In complete contradiction, we show the depolarization ratios of the Arg residues in AP indicate contributions of multiple electronic transitions.

This must be due to the mixing of higher electronic transitions with the peptide bond NV₁ $\pi \rightarrow \pi^*$ transition in AP and with the overlapping broad transition of the guanidinium group. Excitation in this spectral region drives both electronic transitions. This may have important consequences on understanding electron transport in peptides and proteins.

AUTHOR INFORMATION

Corresponding Author

*Phone: 412-624-8570. Fax: 412-624-0588. E-mail: asher@pitt.edu.

ACKNOWLEDGMENT

We thank Dr. Nataliya Myshakina, Zhenmin Hong, and Jonathan Wert for useful discussions. We also thank the NIH for funding, Grant #1R01EB009089.

REFERENCES

- (1) Barnes, D. G.; Rhodes, W. *J. Chim. Phys.* **1968**, *48*, 817.
- (2) Basch, H.; Robin, M. B.; Kuebler, N. A. *J. Chem. Phys.* **1967**, *47*, 1201.
- (3) Basch, H.; Robin, M. B.; Kuebler, N. A. *J. Chem. Phys.* **1968**, *49*, 5007.
- (4) Johnson, W. C., Jr.; Simpson, W. T. *J. Chem. Phys.* **1968**, *48*, 2168.
- (5) Kaya, K.; Nagakura, S. *Theor. Chim. Acta* **1967**, *7*, 117.
- (6) Moffitt, W. *Proc. Natl. Acad. Sci. U.S.A.* **1956**, *42*, 736.
- (7) Moffitt, W. *J. Chem. Phys.* **1956**, *25*, 467.
- (8) Nagakura, S. *Mol. Phys.* **1960**, *3*, 105.
- (9) Peterson, D. L.; Simpson, W. T. *J. Am. Chem. Soc.* **1957**, *79*, 2375.
- (10) Schellman, J. A.; Nielsen, E. B. *J. Phys. Chem.* **1967**, *71*, 3914.
- (11) Woody, R. W. *Monatsh. Chem.* **2005**, *136*, 347.
- (12) Woody, R. W. *J. Am. Chem. Soc.* **2009**, *131*, 8234.
- (13) Woody, R. W. *Chirality* **2010**, *22*, E22.
- (14) Asher, S. A.; Ianoul, A.; Mix, G.; Boyden, M. N.; Karnoup, A.; Diem, M.; Schweitzer-Stenner, R. *J. Am. Chem. Soc.* **2001**, *123*, 11775.
- (15) Asher, S. A.; Mikhonin, A. V.; Bykov, S. *J. Am. Chem. Soc.* **2004**, *126*, 8433.
- (16) Bykov, S.; Asher, S. *J. Phys. Chem. B* **2010**, *114*, 6636.
- (17) Bykov, S. V.; Asher, S. A. *J. Phys. Chem. Lett.* **2010**, *1*, 269.
- (18) Dudik, J. M.; Johnson, C. R.; Asher, S. A. *J. Chem. Phys.* **1985**, *82*, 1732.
- (19) Lednev, I. K.; Karnoup, A. S.; Sparrow, M. C.; Asher, S. A. *J. Am. Chem. Soc.* **1999**, *121*, 8074.
- (20) Ma, L.; Ahmed, Z.; Mikhonin, A. V.; Asher, S. A. *J. Phys. Chem. B* **2007**, *111*, 7675.
- (21) Mikhonin, A. V.; Ahmed, Z.; Ianoul, A.; Asher, S. A. *J. Phys. Chem. B* **2004**, *108*, 19020.
- (22) Mikhonin, A. V.; Bykov, S. V.; Myshakina, N. S.; Asher, S. A. *J. Phys. Chem. B* **2006**, *110*, 1928.
- (23) Shafaat, H. S.; Sanchez, K. M.; Neary, T. J.; Kim, J. E. *J. Raman Spectrosc.* **2009**, *40*, 1060.
- (24) Sharma, B.; Asher, S. A. *J. Phys. Chem. B* **2010**, *114*, 6661.
- (25) Sharma, B.; Bykov, V.; Asher, S. A. *J. Phys. Chem. B* **2008**, *112*, 11762.
- (26) Shi, Z.; Olson, C. A.; Bell, A. J., Jr.; Kallenbach, N. R. *Biopolymers* **2001**, *60*, 366.
- (27) Topilina, N. I.; Ermolenkov, V. V.; Sikirzhitski, V.; Higashiya, S.; Lednev, I. K.; Welch, J. T. *Biopolymers* **2010**, *93*, 607.
- (28) Xiong, K.; Asciutto, E. K.; Madura, J. D.; Asher, S. A. *Biochemistry* **2009**, *48*, 10818.
- (29) Asher, S. A.; Chi, Z.; Li, P. *J. Raman Spectrosc.* **1998**, *29*, 927.
- (30) Asher, S. A.; Ludwig, M.; Johnson, C. R. *J. Am. Chem. Soc.* **1986**, *108*, 3186.
- (31) Chen, X. G.; Asher, S. A.; Schweitzer-Stenner, R.; Mirkin, N. G.; Krimm, S. *J. Am. Chem. Soc.* **1995**, *117*, 2884.
- (32) Chen, X. G.; Li, P.; Holtz, J. S. W.; Chi, Z.; Pajcini, V.; Asher, S. A.; Kelly, L. A. *J. Am. Chem. Soc.* **1996**, *118*, 9716.
- (33) Chen, X. G.; Schweitzer-Stenner, R.; Krimm, S.; Mirkin, N. G.; Asher, S. A. *J. Am. Chem. Soc.* **1994**, *116*, 11141.
- (34) Cho, N.; Asher, S. A. *Biospectroscopy* **1996**, *2*, 71.
- (35) DeVito, V. L.; Cai, M. Z.; Asher, S. A.; Kehres, L. A.; Smith, K. M. *J. Phys. Chem.* **1992**, *96*, 6917.
- (36) Harmon, P. A.; Asher, S. A. *J. Chem. Phys.* **1990**, *93*, 3094.
- (37) Sweeney, J. A.; Asher, S. A. *J. Phys. Chem.* **1990**, *94*, 4784.
- (38) Balakrishnan, G.; Weeks, C. L.; Ibrahim, M.; Soldatova, A. V.; Spiro, T. G. *Curr. Opin. Struct. Biol.* **2008**, *18*, 623.
- (39) Bykov, S.; Lednev, I.; Ianoul, A.; Mikhonin, A.; Munro, C.; Asher, S. A. *Appl. Spectrosc.* **2005**, *59*, 1541.
- (40) Sension, R. J.; Hudson, B.; Callis, P. R. *J. Phys. Chem.* **1990**, *94*, 4015.
- (41) Garfinkel, D. *J. Am. Chem. Soc.* **1958**, *80*, 3827.
- (42) Hernandez, B.; Pfluger, F.; Derbel, N.; De Coninck, J.; Ghomi, M. *J. Phys. Chem. B* **2010**, *114*, 1077.
- (43) Hildebrandt, P.; Czernuszewicz, R. S.; Grygon, C. A.; Spiro, T. G. *J. Raman Spectrosc.* **1989**, *20*, 645.
- (44) Kalaiselvi, D.; Kumar, R. M.; Jayavel, R. *Cryst. Res. Technol.* **2008**, *43*, 851.
- (45) Lima, R. J. C.; Freire, P. T. C.; Sasaki, J. M.; Melo, F. E. A.; Mendes Filho, J. *J. Raman Spectrosc.* **2002**, *33*, 625.
- (46) Ludwig, M.; Asher, S. A. *Appl. Spectrosc.* **1988**, *42*, 1458.
- (47) Shriver, D. F.; Dunn, J. B. R. *Appl. Spectrosc.* **1974**, *28*, 319.
- (48) Hong, Z.; Wert, J.; Asher, S. A. Manuscript in preparation.
- (49) Long, D. A. *The Raman Effect: A Unified Treatment of the Theory of Raman Scattering by Molecules*; John Wiley & Sons: New York, 2001.